sciendo
DOI 10.2478/ama-2025-0021 acta mechanica et automatica, vol.19 no.2 (2025)

EFFECTIVE ROLE OF CUBIC SPLINES FOR THE NUMERICAL COMPUTATIONS OF NON-LINEAR MODEL OF VISCOELASTIC FLUID

Aasma Khalid*, Rubab Batool*, Kashif Ali Abro, Akmal Rehan*****

*Department of Mathematics, GC Women University Faisalabad, 38023, Faisalabad, Pakistan
**Institute of Ground Water Studies, Faculty of Natural and Agricultural Sciences, University of the Free State, South Africa,
Department of Basic Science and Related Studies, Mehran University of Engineering and Technology, Jamshoro, Pakistan,
Faculty of Mathematics and Statistics, Ton Duc Thang University, Ho Chi Minh City,Vietnam
*** Deptartment of Computer Science, University of Agriculture Faisalabad, 38023, Faisalabad, Pakistan

aasmakhalid@gcwuf.edu.pk, rubabbatool1272@gmail.com, kashif.abro@faculty.muet.edu.pk, akmalrehan@uaf.edu.pk

received 05 January 2024, revised 02 June 2024, accepted 25 June 2024

Abstract: The seventh-order boundary value problems (BVPs), which are important because of their complexity and prevalence in many scientific and engineering fields, are the subject of this paper's study. These high-order boundary value problems appear in fields such as fluid dynamics, where they are used to model fluid flow, and in elasticity theory, where they help describe the deformation of materials. Unfortunately, the precision and stability required to solve these high-order problems consistently are frequently lacking from current numerical techniques. Consequently, the advancement of theoretical research as well as practical applications in these disciplines depends on the development of a reliable and accurate method for solving seventh-order boundary value problems. In order to improve the accuracy and stability of solutions for these challenging issues, we propose novel numerical strategies that involves non-polynomial and polynomial cubic splines. For both methods, the domain [0,1] is divided into sub-intervals with step sizes of h=1/10 and h=1/5. This method involves initially transforming the seventh-order boundary value problems into a system of second-order. These second-order boundary value problems are then discretized using finite difference approximations, incorporating essential boundary conditions, and ultimately converted into a set of linear algebraic equations. The employed methods are rigorously assessed through experimentation on three distinct test problems. The outcomes attained showcase an exceptional level of accuracy, extending up to 7 decimal places. These commendable results are vividly depicted in both the tabulated data and accompanying graphs. Such a high degree of precision substantiates the dependability and efficiency of the proposed method. Comparisons, presented in tables and graphs, highlight the precision and reliability of our methods. These comparisons confirm that our approaches are valuable tools for addressing the challenges associated with seventh-order boundary value problems, marking a notable contribution to the field of numerical analysis. While lower-order boundary value problems have been extensively studied, applying these splines methods to seventh-order boundary value problems presents new challenges and insights. The novelty of this work involves non-polynomial and polynomial cubic spline techniques to solve seventh-order boundary value problems, offering improved accuracy and stability over existing numerical methods.

Key words: finite difference method, central difference, boundary value problems, non polynomial, spline methods, polynomial, numerical analysis

1. INTRODUCTION

Seventh-order boundary value problems are not as common as lower-order problems but can arise in specific physical and engineering contexts, particularly in areas where complex phenomena need to be described with high precision. For example, the deflection $y(x)$ of a beam might be described by a seventh-order differential equation to capture detailed physical effects:

$$EI\frac{d^7y}{dx^7}=f(x), \tag{1}$$

where E is the modulus of elasticity, I is the moment of inertia, and $f(x)$ is the distributed load.

In fluid mechanics, seventh-order BVPs describe complex flow patterns and instabilities in boundary layers, such as those found in advanced aerodynamics or wave propagation phenomena:

$$\frac{d^7u}{dx^7}+a\frac{d^5u}{dx^5}+b\frac{d^3u}{dx^3}+cu=0, \tag{2}$$

where u represents the flow variable, and a, b, and c are coefficients representing various physical parameters. In nonlinear dynamics, these equations capture detailed interactions in systems exhibiting chaotic behavior. In quantum mechanics, higher-order differential equations appear in advanced quantum field theories and perturbation analysis, where they describe the behavior of quantum fields under complex interactions.

In computer graphics, dealing with curves is essential for drawing various objects on the screen. Cubic curves, both non-polynomial and polynomial splines, are commonly used due to their flexibility. The novelty of this study lies in the approach of utilizing both CPS and CNPS methods, to tackle nonlinear seventh-order BVPs. While previous research has explored various numerical methods for lower-order BVPs, the application of these spline techniques to seventh-order nonlinear problems is relatively unexplored.

Cubic polynomial splines are widely used due to their smoothness and computational efficiency. They ensure continuity of the first and second derivatives, which is crucial for accurately solving

DOI 10.2478/ama-2025-0021

high-order differential equations. The general form of a cubic spline $S(x)$ between two points x_i and x_{i+1} is:

$$S_i(x) = a_i + b_i(x - x_i) + c_i(x - x_i)^2 + d_i(x - x_i)^3, \tag{3}$$

where a_i, b_i, c_i, and d_i are coefficients determined by the spline conditions, including continuity of the first and second derivatives at the knots.

Nonpolynomial splines, such as trigonometric or exponential splines, offer flexibility in modeling functions with periodic or rapidly varying behavior, which is often encountered in physical problems. For example, a trigonometric spline $T(x)$ might be expressed as:

$$T_i(x) = a_i + b_i \sin(\omega(x - x_i)) + c_i \cos(\omega(x - x_i)), \tag{4}$$

where ω is the frequency parameter, and a_i, b_i, and c_i are coefficients. These splines are particularly useful in handling boundary conditions that exhibit periodicity or oscillatory characteristics.

Despite the advantages of CPS and CNPS methods, there are several limitations to our approach. These methods can become computationally intensive, especially for smaller step sizes, which yield more accurate results but at the cost of increased computational demand. Conversely, larger step sizes may reduce computational effort but compromise accuracy, especially for problems with steep gradients or rapid changes. Implementing cubic polynomial splines can be more complex than using simpler methods like finite differences, requiring careful construction and continuity at the knots. While cubic splines generally provide good convergence properties, certain nonlinear or stiff problems may require very fine discretization to achieve desired accuracy, increasing computational costs.

In [1], the authors conducted extensive research on the solution of parabolic Partial Differential Equations (PDEs). They introduced a novel method for calculating numerical solutions of fourth-order PDEs, building upon the foundation of the polynomial cubic spline method and the Alternating Direction Method (ADM). The ADM approach dismantled the constraints of alternate variables to achieve successive approximations. A solution to a seventh-order BVP using cubic B-spline functions was presented in [2]. The authors propose an efficient numerical algorithm based on cubic B-splines to approximate the solution to the BVP.

In [3], the focus was on trajectory planning for a robotic arm endowed with seven degrees of freedom. The primary goal was to facilitate efficient and seamless targeting of a specified point by the robotic arm. To address this challenge, cubic polynomials and seventh-degree polynomials were harnessed for joint space trajectory planning, all grounded in a foundation of kinematics analysis. The trajectory planning was subsequently simulated utilizing the MATLAB platform, enabling a comprehensive evaluation of its effectiveness and performance.

Mathematicians and engineers historically encountered challenges when attempting to solve higher-order differential equations. To address such complexities and find numerical approximations, a range of numerical techniques were employed. In [4], authors presented a distinctive numerical approach aimed at approximating tenth-order Boundary Value Problems (BVPs). The methods devised within this study were based on the innovative concept of amalgamating the decomposition process with the Non-Polynomial Cubic Spline Method (NPCSM) and the Polynomial Cubic Spline Method (PCSM).

In a research investigation employing the Kernel Hilbert technique, as outlined in [5], the study showcased the method's proficiency in solving seventh-order Boundary Value Problems (BVPs) while adhering to boundary constraints. These findings were then contrasted with those obtained using various approaches, such as HPM, VPM, VIM, ADM, and HAM. In addition, the authors of [6] suggested using the Cubic B spline approach to deal with the numerical solutions of seventh-order BVPs. For a quantitative knowledge of seventh-order BVPs, including both linear and non-linear forms, this work especially used CB splines.

A innovative numerical method was developed in [7] by creating ninth-degree spline functions by using extended cubic splines. This method provided a special answer to challenging mathematical issues. The authors proposed a numerical method for solving linear seventh-order ordinary boundary value problems (BVPs) by utilizing the B-Spline system (BSM) in a separate work, which is described in [8]. The particular traits of seventh-order BVPs served as a foundation for the creation of this approach. In order to approximate the Septic B-Spline formulation, they invented the Collocation BSM, which they used to effectively achieve their goal.

The Homotopy Perturbation Method (HPM) was used by the author in [9] to offer a method for approximating seventh-order linear and nonlinear boundary value problems (BVPs). This approach established itself as a useful tool in this field by demonstrating its capacity to solve higher-order linear and nonlinear BVPs with little absolute error. The authors of [10] concentrated on employing quartic B-spline functions to solve seventh-order BVPs. The authors provided an efficient method for dealing with this kind of issues by proposing a numerical strategy that made use of quartic B-splines to approximate the answers.

In their research [11], the authors employed Non-Polynomial Cubic Splines of Sixth Order in conjunction with Finite Difference Approximations to solve a complex array of linear algebraic equations inherent in Boundary Value Problems (BVPs). The researchers in [12, 13, 16, 18] investigated the application of three mathematical methods, namely the homotopy perturbation method (HPM), cubic spline, spline collocation method, differential transform technique (DTT) and the modified Adomian decomposition method (MADM), for solving higher-order boundary value problems (BVPs). In [14], the author introduced an efficient numerical algorithm for solving seventh-order BVPs. The approach utilized cubic B-spline functions to approximate the solution, offering a reliable method for tackling such higher-order problems. Authors in [15] introduced quintic nonpolynomial spline algorithms specifically tailored for addressing fourth-order two-point BVPs. Importantly, this methodology extended its applicability to encompass Partial Differential Equations (PDEs) up to the fourth order, leading to enhanced approximations while demanding reduced computational effort.

In the study of induction motors [17], the behavior could be accurately described by a fifth-order differential equation (DE) model. By incorporating a torque correction factor, the full seventh-order DE structure faithfully replicated the transient torques as well as the instantaneous real and reactive power flows. Seventh-order Boundary Value Problems (BVPs) were solved using He's polynomials and the Variational Iteration Method (VIM). The solutions to these problems were approximated using a rapidly converging series.

The transformation of seventh-order Boundary Value Problems (BVPs) into a set of Integral Equations (IE) was demonstrated in [19, 20], and these equations were solvable using the Variational Element Method (VEM). It's worth noting that, at that time, there was no literature available on the numerical solutions to seventh-order BVPs and related Eigenvalue Problems (EVP). The approximate solutions of these equations were expressed in terms of overlapping series with calculable elements. By combining the Homotopy Perturbation Method (HPM) and the Adomian Decomposition Method

(ADM), [21] was able to solve seventh-order BVPs. The writers were able to solve the difficulties precisely and quickly by the use of this method. A method for solving seventh-order BVPs using cubic trigonometric B-spline functions was provided by the authors in [22]. Their approach provided an effective strategy to deal with such high-order BVPs by approximating the solutions using these customized B-splines. The author of [23] developed a numerical strategy for quickly solving linear fourth-order boundary value problems (BVPs) using the Non-Polynomial Spline (NPS) technique.

1.1. Basics of Cubic Non-Polynomial Splines

Let's break the interval [a, b] into n small intervals by using node points: $\varpi_e = a + eh$, where e = 0, 1, ..., n, where $a = \varpi_0$ and $b = \varpi_n$ with the step size $h = \frac{b-a}{n}$ and n is a positive integer. Let $\chi(\varpi)$ be the precise solution and χ_e be an estimate to $\chi(\varpi_e)$ attained by the CNPS $X_e(\varpi)$ between the points (ϖ_e, χ_e) and $(\varpi_{e+1}, \chi_{e+1})$. It is necessary for $X_e(\varpi)$ to fulfill the ICs at ϖ_e and ϖ_{e+1}, the BCs, and in the same way, the continuity of the initial derivative at the collective points (ϖ_e, s_e). For every part (ϖ_e, ϖ_{e+1}) where e = 0, 1, 2, 3, 4, ..., n-1, the spline $X_e(\varpi)$ makes the form:

$$X_e(\varpi) = q_e + l_e(\varpi - \varpi_e) + s_e \sin\sigma(\varpi - \varpi_e) + n_e \cos\sigma(\varpi - \varpi_e) \tag{5}$$

where q_e, l_e, s_e, and n_e are constants and σ is a free quantity.

A NP function X_ϖ of class $R^2[a,b]$ which includes χ_ϖ at the node points ϖ_e; e = 0, 1, 2, 3, 4, ..., n is influenced by a parameter σ and decreases to a Cubic-Spline X_ϖ in $[a,b]$ as σ approaches 0. For the derivation of the coefficient of the equation (5) in terms of $\chi_e, \chi_{e+1}, N_e, N_{e+1}$, we first define:

$$X_e(\varpi_e) = \chi_e, \quad X_e(\varpi_{e+1}) = \chi_{e+1} \tag{6}$$

The consequent expression for the equation (5) is obtained by straightforward algebraic manipulation:

$$q_e = \chi_e + \frac{N_e}{\sigma^2}, \quad l_e = \frac{\chi_{e+1} - \chi_e}{h} + \frac{N_{e+1} - N_e}{\zeta\theta}$$

$$s_e = \frac{N_e \cos\theta - N_{e+1}}{\sigma^2 \sin\theta}, \quad n_e = -\frac{N_e}{\sigma^2}$$

where $\theta = Nh$. By the continuity equation of the first derivative at node point (ϖ_e, χ_e), i.e., $X'_{e-1}(\varpi_e) = X'_e(\varpi_e)$ is the consistency relation for e = 0, 1, ..., n-1:

$$\zeta(N_{e+1} + N_{e-1}) + 2\delta(N_e) = \frac{1}{h^2}(\chi_{e-1} + \chi_{e+1} - 2\chi_e) \tag{7}$$

where we've inserted:

$$\zeta = \frac{1}{\theta \sin\theta} - \frac{1}{\theta^2}, \quad \delta = \frac{-1}{\theta^2} - \frac{-\cos\theta}{\theta}, \quad \chi'' = N \tag{8}$$

and $\theta = Nh$

The described approach is 4th order convergent if $1\text{-}2\zeta\text{-}2\delta=0$ and $\zeta=\frac{1}{12}$ [23].

1.2. Basics of Cubic Polynomial Splines

Let's break the interval [a, b] into n small intervals by using nodepoints: $\varpi_e = a + eh, e = 0,1,2,3,4,\dots,n$ where $a = \varpi_0$, $b = \varpi_n$ with the step size $h = \frac{b-a}{n}$ and n a positive integer.

Let $\chi(\varpi)$ be the precise solution and χ_e be an estimate to $\chi(\varpi_e)$ attained by the NPS $X_e(\varpi)$ between the points (ϖ_e, χ_e) and $(\varpi_{e+1}, \chi_{e+1})$. It is necessary for $X_e(\varpi)$ to fulfill the interpolating conditions at ϖ_e and ϖ_{e+1}, the BCs, and in the same way, the continuity of the initial derivative at the collective points (ϖ_e, χ_e). For every part (ϖ_e, ϖ_{e+1}) where e = 0, 1, 2, 3, 4, ..., n-1 the spline $X_e(\varpi)$ makes the form where q_e, l_e, s_e, and n_e are constants and σ is a free quantity.

A NP function X_ϖ of class $R^2[a,b]$ which includes χ_ϖ at the node points ϖ_e; e = 0, 1, 2, 3, 4, ..., n be influenced by a parameter σ and decreases to a Cubic-Spline X_ϖ in [a, b] as σ approaches 0. We first define:

$$X_e(\varpi_e) = \chi_e, \quad X_e(\varpi_{e+1}) = \chi_{e+1}, \quad X''_e(\chi_e) = N_e, \quad X''_e(\chi_{e+1}) = N_{e+1} \tag{9}$$

By using a straightforward algebraic operation, we may get the corresponding expression:

$$q_e = \chi_e + \frac{N_e}{\sigma^2}, \quad l_e = \frac{\chi_{e+1} - \chi_e}{h} + \frac{N_{e+1} - N_e}{\zeta\theta}$$

$$s_e = \frac{N_e \cos\theta - N_{e+1}}{\sigma^2 \sin\theta}, \quad n_e = -\frac{N_e}{\sigma^2}$$

where

$$\theta = Nh$$

By the continuity equation of the first derivative at node point (ϖ_e, χ_e), i.e., $X'_{e-1}(\varpi_e) = X'_e(\varpi_e)$ is the consistency relation for e = 0, 1, 2, 3, 4, ..., n-1:

$$(N_{e+1} + N_{e-1} + 4N_e) = \frac{6}{h^2}(\chi_{e-1} + \chi_{e+1} - 2\chi_e) \tag{10}$$

where we have substituted:

$$\chi'' = N$$

The paper progresses logically from theory to application. Section 2 discusses the development of CPS and CNPS, while Section 3 evaluates their effectiveness in resolving 7th order BVPs. Section 4 concludes with a concise analysis and recommendations, providing a clear and educational reading experience.

2. SEVENTH ORDER NON-LINEAR BVPS

Using the CPS and CNPS approaches to approximatively solve a nonlinear seventh-order boundary value problem (7^{th} order BVP) is the main goal in this situation. These methods are computational tools designed to generate approximative numerical solutions to this difficult problem. By employing these techniques, we aim to effectively manage the challenges posed by the nonlinear nature of the problem and give exact numerical estimates for the desired outputs.

$$\chi^{(7)}(\varpi) = z(\varpi, \chi(\varpi), \chi^{(1)}(\varpi), \chi^{(2)}(\varpi), \chi^{(3)}(\varpi), \chi^{(4)}(\varpi), \chi^{(5)}(\varpi), \chi^{(6)}(\varpi)); \quad \varpi \epsilon [a,b] \tag{11}$$

along with BCs:

$$\chi^{(2i)}(a) = \zeta_i, \quad \chi^{(2i)}(b) = \delta_i \tag{12}$$

where ζ_i,δ_i; i=0,1,2,3 are constants and ζ_i(o),i=1,...,7 and $z(\varpi)$ are continuous functions on [r,s]. To estimate CNPS and CPS choose S to BVPs with BCs, Let us distribute interval $[r,s]$ into n sub-interval z_i=r+ih, i=0,1,...,n-1,n. $r = z_0$, $s = z_n$, $h = \frac{s-r}{n}$

DOI 10.2478/ama-2025-0021

Now for CNPS $S'_{i-1}(z_i) = S'_i(z_i)$ is relation

$i = 0,1,\ldots,\ n-1,$

$$\zeta\ N_{i+1} + 2\ \delta\ N_i + \ \zeta\ N_{i-1} = \ \frac{1}{h^2}\ (v_{i+1} - 2\ v_i + v_{i-1}) \tag{13}$$

here the substitution

$\zeta = \frac{1}{\theta\ sin\theta} - \frac{1}{\theta^2},\quad \delta = -\frac{1}{\theta^2} - \frac{cos\theta}{\theta}, and\quad \theta = \mho\ h$

Now for CPS $S'_{i-1}(z_i) = S'_i(z_i)$ is relation

$i = 0,1,\ldots,\ n-1,$

$$N_{i+1} + 4N_i + N_{i-1} = \frac{6}{h^2}(v_{i+1} - 2v_i + v_{i-1}) \tag{14}$$

where we have replace

$v'' = N$

Now differentiating (11) w.r.t. χ so, the equation become

$$\chi^{(8)}(\varpi) = z(\varpi, \chi(\varpi), \chi^{(1)}(\varpi), \chi^{(2)}(\varpi), \chi^{(3)}(\varpi), \chi^{(4)}(\varpi), \chi^{(5)}(\varpi), \chi^{(6)}(\varpi), \chi^{(7)}(\varpi)) \tag{15}$$

Equation (15) presents an eighth-order boundary value problem. In order to manage its complexity, we proceeded to transform equation (15) into a system of second-order Boundary Value Problems (BVPs), incorporating the Boundary Conditions (BCs) from equation (12). This transformation was accomplished by substituting the equation into a specific form, resulting in a more manageable representation.

$$\chi''(\varpi) = e(\varpi) \tag{16}$$

$$e''(\varpi) = f(\varpi) \tag{17}$$

$$f''(\varpi) = g(\varpi) \tag{18}$$

in equation (15),the reduced system of 2nd order will be

$$p^{(2)}(k) = z(\varpi, \chi(\varpi), \chi^{(1)}(\varpi), e(\varpi), e^{(1)}(\varpi), f(\varpi), f^{(1)}(\varpi), g(\varpi), g^{(1)}(\varpi));\quad \varpi\epsilon[a, b] \tag{19}$$

Along with boundary conditions:

$$\begin{aligned} &\chi(a) = \zeta_0,\quad \chi(b) = \delta_0\\ &e(a) = \zeta_1,\quad e(b) = \delta_1\\ &f(a) = \zeta_2,\quad f(b) = \delta_2\\ &g(a) = \zeta_3,\quad g(b) = \delta_3 \end{aligned} \tag{20}$$

2.1. Cubic Non-Polynomial Spline

We get relations for $\chi(\varpi)$,$e(\varpi)$,$f(\varpi)$ and $g(\varpi)$ by using the continuity condition of first order derivative, respectively as:

$$\zeta(R_{i+1} + R_{i-1}) + \delta 4R_i = \frac{1}{h^2}(\chi_{i+1} - 2\chi_i + \chi_{i-1}) \tag{21}$$

$$\zeta(S_{i+1} + S_{i-1}) + \delta 4S_i = \frac{1}{h^2}(e_{i+1} - 2e_i + e_{i-1}) \tag{22}$$

$$\zeta(P_{i+1} + P_{i-1}) + \delta 4P_i = \frac{1}{h^2}(g_{i+1} - 2g_i + g_{i-1}) \tag{23}$$

we have substitute

$$\begin{aligned} &\chi''(\varpi) = R(\varpi),\quad e''(\varpi) = S(\varpi),\\ &f''(\varpi) = T(\varpi),\quad g''(\varpi) = P(\varpi) \end{aligned} \tag{24}$$

Discretize equations (15)-(18) at gird points

$(\varpi_i, g_i), (\varpi_i, \chi_i), (\varpi_i, e_i), (\varpi_i f_i)$

$$g^{(2)}(\varpi) = z(\varpi, \chi(\varpi), \chi^{(1)}(\varpi), e(\varpi), e^{(1)}(\varpi), f(\varpi), f^{(1)}(\varpi), g(\varpi), g^{(1)}(\varpi)) \tag{25}$$

$$\begin{aligned} &\chi''(\varpi_i) = e(\varpi_i) = e_i,\\ &e''(\varpi_i) = f(\varpi_i) = f_i,\\ &f''(\varpi_i) = g(\varpi_i) = g_i, \end{aligned} \tag{26}$$

Now after substitution we get

$$\begin{aligned} &\chi''_i = R_i,\quad e''_i = S_i,\\ &f''_i = T_i,\quad g''_i = P_i \end{aligned} \tag{27}$$

then above equation become

$$P_i = z(\varpi_i, \chi(\varpi_i), \chi^{(1)}(\varpi_i), e(\varpi_i), e^{(1)}(\varpi_i), f(\varpi_i), f^{(1)}(\varpi_i), g(\varpi_i), g^{(1)}(\varpi_i)); \tag{28}$$

$$\left.\begin{aligned} &R_i = e_i,\\ &S_i = f_i,\\ &T_i = g_i, \end{aligned}\right\} \tag{29}$$

From equation (28) and (29)

$$P_{i+1} = z(\varpi_{i+1}, \chi(\varpi_{i+1}), \chi^{(1)}(\varpi_{i+1}), e(\varpi_{i+1}), e^{(1)}(\varpi_{i+1}), f(\varpi_{i+1}), f^{(1)}(\varpi_{i+1}), g(\varpi_{i+1}), g^{(1)}(\varpi_{i+1})); \tag{30}$$

$$\left.\begin{aligned} &R_{i+1} = e_{i+1},\\ &S_{i+1} = f_{i+1},\\ &T_{i+1} = g_{i+1}, \end{aligned}\right\} \tag{31}$$

then similarly

$$P_{i-1} = z(\varpi_{i-1}, \chi(\varpi_{i-1}), \chi^{(1)}(\varpi_{i-1}), e(\varpi_{i-1}), e^{(1)}(\varpi_{i-1}), f(\varpi_{i-1}), f^{(1)}(\varpi_{i-1}), g(\varpi_{i-1}), g^{(1)}(\varpi_{i-1})); \tag{32}$$

$$\left.\begin{aligned} &R_{i-1} = e_{i-1},\\ &S_{i-1} = f_{i-1},\\ &T_{i-1} = g_{i-1}, \end{aligned}\right\} \tag{33}$$

The subsequent $O(h^2)$ approximations for the first-order derivatives l, e, f, and g in Equations (28), (30), and (33) offer a viable approach. These approximations can be effectively utilized to enhance the accuracy of the calculations.

$$\left.\begin{aligned} &\chi'_i = \frac{\chi_{i+1} - \chi_{i-1}}{2h},\quad \chi'_{i+1} = \frac{3\chi_{i+1} - 4\chi_i + \chi_{i-1}}{2h},\quad \chi'_{i-1} = \frac{-\chi_{i+1} + 4\chi_i - 3\chi_{i-1}}{2h},\\ &e'_i = \frac{e_{i+1} - e_{i-1}}{2h},\quad e'_{i+1} = \frac{3e_{i+1} - 4e_i + e_{i-1}}{2h},\quad e'_{i-1} = \frac{-e_{i+1} + 4e_i - 3e_{i-1}}{2h},\\ &f'_i = \frac{f_{i+1} - f_{i-1}}{2h},\quad f^{(1)}_{i+1} = \frac{3f_{i+1} - 4f_i + f_{i-1}}{2h},\quad f'_{i-1} = \frac{-f_{i+1} + 4f_i - 3f_{i-1}}{2h},\\ &g'_i = \frac{g_{i+1} - g_{i-1}}{2h},\quad g'_{i+1} = \frac{3g_{i+1} - 4g_i + g_{i-1}}{2h},\quad g'_{i-1} = \frac{-g_{i+1} + 4g_i - 3g_{i-1}}{2h}, \end{aligned}\right\} \tag{34}$$

Using equations (28)-(34) in equations (14) and (21)-(23

$$\left.\begin{aligned} &\zeta e_{i-1} + 2\delta e_i + \zeta e_{i+1} = \frac{1}{h^2}(\chi_{i-1} - 2\chi_i + \chi_{i+1})\\ &\zeta f_{i-1} + 2\delta f_i + \zeta f_{i+1} = \frac{1}{h^2}(e_{i-1} - 2e_i + e_{i+1})\\ &\zeta g_{i-1} + 2\delta g_i + \zeta g_{i+1} = \frac{1}{h^2}(f_{i-1} - 2f_i + f_{i+1}) \end{aligned}\right\} \tag{35}$$

we get

$$\zeta z(\varpi_{i+1}, \chi(\varpi_{i+1}), \chi^{(1)}(\varpi_{i+1}), e(\varpi_{i+1}), e^{(1)}(\varpi_{i+1}), f(\varpi_{i+1}), f^{(1)}(\varpi_{i+1}), g(\varpi_{i+1}), g^{(1)}(\varpi_{i+1})) + 2\delta z(\varpi_i, \chi(\varpi_i), \chi^{(1)}(\varpi_i), e^{(1)}(\varpi_i), f(\varpi_i), f^{(1)}(\varpi_i), g(\varpi_i), g^{(1)}(\varpi_i)) + \zeta z(\varpi_{i-1}, \chi(\varpi_{i-1}), \chi^{(1)}(\varpi_{i-1}), e(\varpi_{i-1}), e^{(1)}(\varpi_{i-1}), f(\varpi_{i-1}), f^{(1)}(\varpi_{i-1}), g(\varpi_{i-1}), g^{(1)}(\varpi_{i-1})) = \frac{1}{h^2}(g_{i-1} - 2g_i + g_{i+1}) \tag{36}$$

we obtain

$$\begin{aligned}
&\zeta z(\varpi_{i+1},\chi(\varpi_{i+1}),\tfrac{3\chi_{i+1}-4\chi_i+\chi_{i-1}}{2h},e(\varpi_{i+1}),\\
&\tfrac{3e_{i+1}-4e_i+e_{i-1}}{2h},f(\varpi_{i+1}),\tfrac{3f_{i+1}-4f_i+f_{i-1}}{2h},g(\varpi_{i+1}),\\
&\tfrac{3g_{i+1}-4g_i+g_{i-1}}{2h}+2\delta z(\varpi_i,\chi(\varpi_i),\tfrac{\chi_{i+1}-\chi_{i-1}}{2h},\\
&e(\varpi_i),\tfrac{e_{i+1}-e_{i-1}}{2h},f(\varpi_i),\tfrac{f_{i+1}-f_{i-1}}{2h},g(\varpi_i),\\
&\tfrac{g_{i+1}-g_{i-1}}{2h}+\zeta z(\varpi_{i-1},\chi(\varpi_{i-1}),\tfrac{-\chi_{i+1}+4\chi_i-3\chi_{i-1}}{2h},\\
&e(\varpi_{i-1}),\tfrac{-e_{i+1}+4e_i-3e_{i-1}}{2h},f(\varpi_{i-1}),\tfrac{-f_{i+1}+4f_i-3f_{i-1}}{2h},\\
&g(\varpi_{i-1}),\tfrac{-g_{i+1}+4g_i-3g_{i-1}}{2h}=\tfrac{1}{h^2}(g_{i-1}-2g_i+g_{i+1})
\end{aligned} \tag{37}$$

Equations (36) and (37), along with the prescribed Boundary Conditions (20), come together to establish a coherent system consisting of $4(n+1)$ equations. Similarly, this system is closely linked to $4(n+1)$ unknowns, showcasing a harmonious synchronization between the equations and the set of unknown constants.

2.2. Cubic Polynomial Spline

We get relations for χ,e,f by make use of flow the surrounding of first order derivative, respectively as

$$\left.\begin{aligned}
(R_{i+1}+R_{i-1})+\delta 4R_i&=\tfrac{6}{h^2}(\chi_{i+1}-2\chi_i+\chi_{i-1})\\
(S_{i+1}+S_{i-1})+\delta 4S_i&=\tfrac{6}{h^2}(e_{i+1}-2e_i+e_{i-1})\\
(P_{i+1}+P_{i-1})+\delta 4P_i&=\tfrac{6}{h^2}(g_{i+1}-2g_i+g_{i-1})
\end{aligned}\right\} \tag{38}$$

After substitution we get

$$\left.\begin{aligned}
\zeta e_{i-1}+2\delta e_i+\zeta e_{i+1}&=\tfrac{6}{h^2}(\chi_{i-1}-2\chi_i+\chi_{i+1})\\
\zeta f_{i-1}+2\delta f_i+\zeta f_{i+1}&=\tfrac{6}{h^2}(e_{i-1}-2e_i+e_{i+1})\\
\zeta g_{i-1}+2\delta g_i+\zeta g_{i+1}&=\tfrac{6}{h^2}(f_{i-1}-2f_i+f_{i+1})
\end{aligned}\right\} \tag{39}$$

By considering the above data NPCS was settled in section, PCS scheme for $i=0,1,\dots,n-1$

Equations (40) and (41) form a system of $4(n+1)$ equations when integrated with Boundary Conditions (20). This system exhibits its smooth interaction and corresponds to a set of $4(n+1)$ unknowns that are interrelated with the $4(n+1)$ equations.

$$\begin{aligned}
&z(m_{i+1},\chi(\varpi_{i+1}),\chi^{(1)}(\varpi_{i+1}),e(\varpi_{i+1}),\\
&e^{(1)}(\varpi_{i+1}),f(\varpi_{i+1}),f^{(1)}(\varpi_{i+1}),g(\varpi_{i+1}),\\
&g^{(1)}(\varpi_{i+1}))+4z(\varpi_i,\chi(\varpi_i),\chi^{(1)}(\varpi_i),e(\varpi_i),\\
&e^{(1)}(\varpi_i),f(\varpi_i),f^{(1)}(\varpi_i),g(\varpi_i),g^{(1)}(\varpi_i))\\
&+z(\varpi_{i-1},\chi(\varpi_{i-1}),\chi^{(1)}(\varpi_{i-1}),e(\varpi_{i-1}),e^{(1)}(\varpi_{i-1}),\\
&f(\varpi_{i-1}),f^{(1)}(\varpi_{i-1}),g(\varpi_{i-1}),\\
&g^{(1)}(\varpi_{i-1}))=\tfrac{6}{h^2}(g_{i-1}-2g_i+g_{i+1})
\end{aligned} \tag{40}$$

and

$$\begin{aligned}
&z(\varpi_{i+1},\chi(\varpi_{i+1}),\tfrac{3\chi_{i+1}-4\chi_i+\chi_{i-1}}{2h},e(\varpi_{i+1}),\\
&\tfrac{3e_{i+1}-4e_i+e_{i-1}}{2h},f(\varpi_{i+1}),\tfrac{3f_{i+1}-4f_i+f_{i-1}}{2h},\\
&g(\varpi_{i+1}),\tfrac{3g_{i+1}-4g_i+g_{i-1}}{2h}+4z(\varpi_i,\chi(\varpi_i),\\
&\tfrac{\chi_{i+1}-\chi_{i-1}}{2h},e(\varpi_i),\tfrac{e_{i+1}-e_{i-1}}{2h},f(\varpi_i),\\
&\tfrac{f_{i+1}-f_{i-1}}{2h},g(\varpi_i),\tfrac{g_{i+1}-g_{i-1}}{2h}+z(\varpi_{i-1},\\
&\chi(\varpi_{i-1}),\tfrac{-\chi_{i+1}+4\chi_i-3\chi_{i-1}}{2h},e(\varpi_{i-1}),\\
&\tfrac{-e_{i+1}+4e_i-3e_{i-1}}{2h},f(\varpi_{i-1}),\tfrac{-f_{i+1}+4f_i-3f_{i-1}}{2h},\\
&g(\varpi_{i-1}),\tfrac{-g_{i+1}+4g_i-3g_{i-1}}{2h}=\tfrac{6}{h^2}(g_{i-1}-2g_i+g_{i+1})
\end{aligned} \tag{41}$$

3. NUMERICAL RESULTS AND DISCUSSIONS

This section explores the outcomes of using CPS and CNPS methods to approximate solutions for a nonlinear seventh-order Boundary Value Problem (7^{th} BVP). By choosing step sizes $h=1/10$ and $h=1/5$, we examine their impact on accuracy and computational efficiency. Smaller step sizes often yield more precise results but increase computational demands, highlighting the trade-off between accuracy and processing power. Comparing results across different step sizes provides insights into the convergence behavior and efficiency of both methods, demonstrating how they adapt to the complexities of the nonlinear 7^{th} order BVP. This analysis sheds light on their convergence characteristics and offers practical guidance on balancing accuracy and computational efficiency in solving complex mathematical problems.

The solution process for the given boundary value problem involves several steps. Problem 3.1/3.2/3.3 was compared with equation (11) and boundary conditions with (12). Then, continuity conditions are defined to ensure smooth transitions across the intervals of the problem domain. Coefficients required for the numerical solution are then derived based on the given differential equation and boundary conditions by discretizing equations (15)-(18) at gird points $(\varpi_i,g_i),(\varpi_i,\chi_i),(\varpi_i,e_i),(\varpi_i f_i)$. The subsequent $O(h^2)$ approximations for the first-order derivatives l, e, f, and g in Equations (28), (30), and (33) offer a viable approach. These approximations can be effectively utilized to enhance the accuracy of the calculations. Consistency relations prepared following the equations 34 are verified to ensure the accuracy of the numerical method. The resulting system of equations Using equations (28)-(35) in equations (14) and (21)-(23) is obtained and we get equations (36-37) then we solved numerically, and higher-order boundary value problems are transformed into a system of second-order differential equations. This transformed system is discretized, preparing it for numerical approximation and Equations (36) and (37), along with the prescribed Boundary Conditions (20), come together to establish a coherent system consisting of 44 equations for $h=0.1$ and 24 equations for $h=0.2$.

Similarly, this system is closely linked to 44 unknowns for $h=0.1$ and 24 unknowns for $h=0.2$, showcasing a harmonious synchronization between the equations and the set of unknown constants. The numerical solution is then obtained using appropriate numerical methods. Finally, the process concludes, having successfully approximated the solution to the given boundary value problem for CNPS. By considering the above data CNPS was settled in section, CPS scheme for $i=0,1,\dots,n-1$ will be developed using equations 38-39. Equations (40) and (41) form a system of $4(n+1)$ equations when integrated with Boundary Conditions (20). This system exhibits smooth interaction and corresponds to a set of 44 unknowns for $h=0.1$ and 24 unknowns for $h=0.2$ unknowns that are interrelated with the 44 equations for $h=0.1$ and 24 equations for $h=0.2$.

3.1 Problem 3.1

Consider the nonlinear BVP

$$\chi^{(7)}(\varpi)=-e^{\varpi}(w(\varpi))^2 \quad 0\le\varpi\le 1$$

subject to

$$\chi^{(n)}(0)=1,\quad \chi^{(n)}(1)=e^{-1}$$

for $n=0,2,4,6$.

The precise solution to the problem under consideration is

DOI 10.2478/ama-2025-0021

mathematically defined as $\chi(\varpi) = e^{-\varpi}$. In order to rigorously validate and assess the efficacy of the proposed method, a systematic evaluation was conducted. The interval $[0,1]$ was strategically divided into sub-intervals, employing both 10 and 5 equal segments. Subsequently, the CPS and CNPS techniques were employed to approximate the solution within each of these sub-intervals.

The outcomes obtained from the CPS and CNPS methods were meticulously compared against the analytically derived solution. For a finer granularity, the results were organized and presented in a clear tabular format. Specifically, Tab.1 was employed to present the numerical outcomes when the step size was set at $h = \frac{1}{10}$, and Tab. 2 for the case when $h = \frac{1}{5}$.

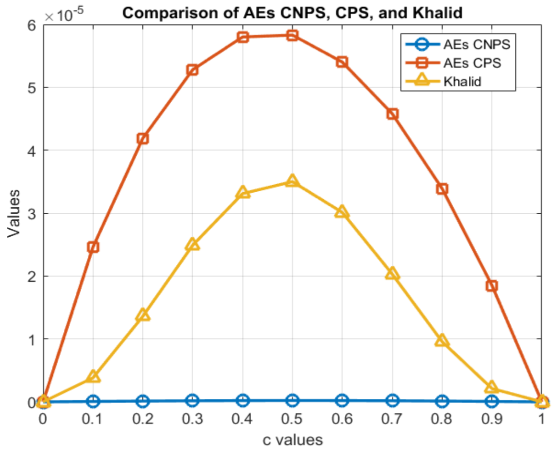

Fig.1. Comparison of AEs of CNPS and CPS with [6] of problem 3.1 at $h = \frac{1}{10}$

In addition to the numerical comparisons, visual aids were also harnessed to provide a more intuitive understanding of the precision achieved by the CPS and CNPS methods. To this end, Fig.1 and Fig.2 are crafted to illustrate the absolute errors associated with the chosen splines, specifically focusing on the scenario when the step size was $h = \frac{1}{10}$.

3.2 Problem 3.2

Consider the nonlinear BVP

$\chi^7(\varpi) = \chi(\varpi)\chi'(\varpi) + e^{-2\varpi}(2 + e^{\varpi}(\varpi - 8) - 3\varpi + \varpi^2)0 \leq \varpi \leq 1$

subject to

$\chi^{(n)}(0) = (-1)^{\frac{n}{2}}(n+1), \quad \chi^{(n)}(1) = (-1)^{\frac{n}{2}}(n+1)e$ for $n = 0,2,4,6$.

The precise solution is given as $\chi(\varpi) = (1-\varpi)e^{-\varpi}$. To assess the performance of the proposed method, we conducted a systematic evaluation by segmenting the interval $[0,1]$ into 10 and 5 equal sub-intervals. Subsequently, we applied the CPS and CNPS methods to generate numerical outcomes, which were then juxtaposed with the specific analytical solution. These comparative analyses are exhaustively presented in Tab.3 for a step size of $h = \frac{1}{10}$ and in Tab.4 for $h = \frac{1}{5}$.

In order to offer a more intuitive insight into the precision achieved, Fig.3 and Fig.4 are constructed to visually depict the absolute errors associated with the employed splines when $h = \frac{1}{10}$. These graphical representations enhance clarity by providing a visual representation of how closely the CPS and CNPS methods correspond to the analytical solution.

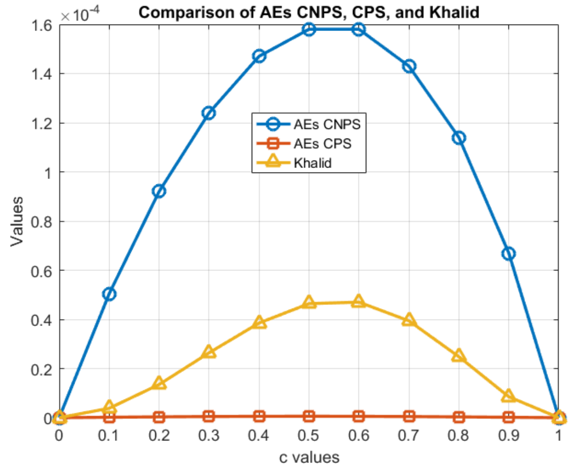

Fig.3. Comparison of AEs of CNPS and CPS with [6] of problem 3.2 at $h = \frac{1}{10}$

3.3 Problem 3.3

Consider the nonlinear BVP $\chi^{(7)} = e^{-\varpi}(w(\varpi))^2 \quad 0 \leq \varpi \leq 1$ subject to $\chi^{(n)}(0) = 1, \quad \chi^{(n)}(1) = e^1$ for $n = 0,2,4,6$.

In pursuit of accurate approximations, the sought-after solution is $\chi(\varpi) = e^{\varpi}$. To rigorously examine the effectiveness of the proposed method, a meticulous analysis was undertaken. The interval $[0,1]$ was thoughtfully divided into 10 and 5 equal sub-intervals, setting the stage for a granular evaluation. By applying the CPS and CNPS methods, numerical results were obtained and subjected to a direct comparison with the precise analytical solution. These insightful evaluations are meticulously presented in Tab.5 for a step size of $h = \frac{1}{10}$ and in Tab.6 for $h = \frac{1}{5}$.

For an enhanced grasp of the achieved precision, Fig.5 and Fig.6 are crafted to visually encapsulate the absolute errors tied to the utilized splines, specifically when $h = \frac{1}{10}$. These graphical representations serve as a powerful tool for gauging the closeness of the CPS and CNPS methods to the established analytical solution.

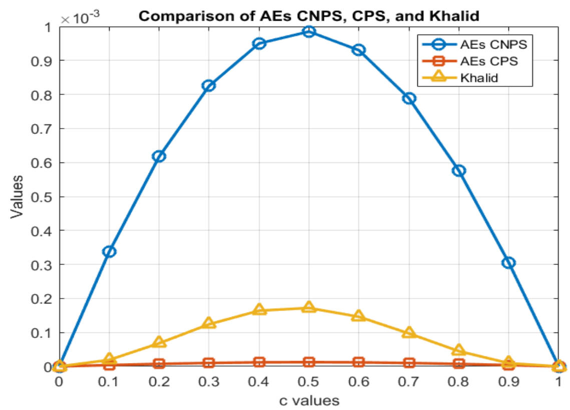

Fig.5. Comparison of AEs of CNPS and CPS with [6] of problem 3.3 at $h = \frac{1}{10}$

DOI 10.2478/ama-2025-0021

Tab.1. Comparison of accurate, CNPS along with CPS for problem 3.1 at $h=\frac{1}{5}$

ϖ	Accurate solution	CNPS solution	$\lvert error \rvert$ on CNPS	CPS solution	$\lvert error \rvert$ on CPS
0	1	1	0.00E-00	1	0.00E-00
0.2	0.818730753	0.817688874	1.04E-03	0.817618382	1.11E-03
0.4	0.670320046	0.668633087	1.69E-03	0.668558559	1.76E-03
0.6	0.548811636	0.547122919	1.69E-03	0.547064978	1.75E-03
0.8	0.449328964	0.448284237	1.04E-03	0.448246958	1.08E-03
1	0.367879441	0.367879441	0.00E-00	0.367879441	0.00E-00

Tab. 2. Comparison of accurate, CNPS along with CPS for problem 3.1 at $h=\frac{1}{10}$

ϖ	Accurate solution	CNPS solution	$\lvert error \rvert$ on CNPS	CPS solution	$\lvert error \rvert$ on CPS	[6]
0	1	1	0.00E-00	1	0.00E-00	0.00E-00
0.1	0.904837418	0.904837481	6.27E-08	0.904812814	2.46E-05	3.82E-06
0.2	0.818730753	0.818730875	1.22E-07	0.818688854	4.19E-05	1.36E-05
0.3	0.740818221	0.740818391	1.70E-07	0.740765438	5.28E-05	2.49E-05
0.4	0.670320046	0.670320248	2.02E-07	0.670262025	5.80E-05	3.31E-05
0.5	0.60653066	0.606530874	2.14E-07	0.606472401	5.83E-05	3.50E-05
0.6	0.548811636	0.548811841	2.05E-07	0.548757603	5.40E-05	3.01E-05
0.7	0.496585304	0.496585478	1.74E-07	0.496539521	4.58E-05	2.03E-05
0.8	0.449328964	0.44932909	1.26E-07	0.449295105	3.39E-05	9.57E-06
0.9	0.40656966	0.406569726	6.61E-08	0.406551127	1.85E-05	2.11E-06
1	0.367879441	0.367879441	0.00E-00	0.367879441	0.00E-00	0.00E-00

Tab. 3. Comparison of accurate, CNPS along with CPS for problem 3.2 at $h=\frac{1}{5}$

ϖ	Accurate solution	CNPS solution	$\lvert error \rvert$ on CNPS	CPS solution	$\lvert error \rvert$ on CPS
0	1	1	0.00E-00	1	0.00E-00
0.2	0.654984602	0.654548343	4.36E-04	0.653822489	1.16E-03
0.4	0.402192028	0.401485267	7.07E-04	0.400509549	1.68E-03
0.6	0.219524654	0.218816219	7.08E-04	0.217928602	1.60E-03
0.8	0.089865793	0.089426899	4.39E-04	0.088878968	9.87E-04
1	0	0	0.00E-00	0	0.00E-00

Tab. 4. Comparison of accurate, CNPS along with CPS for problem 3.2 at $h=\frac{1}{10}$

ϖ	Accurate solution	CNPS solution	$\lvert error \rvert$ on CNPS	CPS solution	$\lvert error \rvert$ on CPS	[6]
0	1	1	0.00E-00	1	0.00E-00	0.00E-00
0.1	0.814353676	0.814349741	0.814016517	3.37E-04	3.94E-06	1.91E-05
0.2	0.654984602	0.654977145	0.654367593	6.17E-04	7.46E-06	6.81E-05
0.3	0.518572754	0.518562529	0.517747628	8.25E-04	1.02E-05	1.24E-04
0.4	0.402192028	0.402180054	0.401241892	9.50E-04	1.20E-05	1.64E-04
0.5	0.30326533	0.303252787	0.302279968	9.85E-04	1.25E-05	1.72E-04
0.6	0.219524654	0.219512766	0.218594693	9.30E-04	1.19E-05	1.46E-04
0.7	0.148975591	0.148965506	0.148186139	7.89E-04	1.01E-05	9.70E-05
0.8	0.089865793	0.089858479	0.089290229	5.76E-04	7.31E-06	4.49E-05
0.9	0.040656966	0.040653124	0.040351558	3.05E-04	3.84E-06	9.44E-06
1	0	0	0	0.00E-00	0.00E-00	0.00E-00

DOI 10.2478/ama-2025-0021

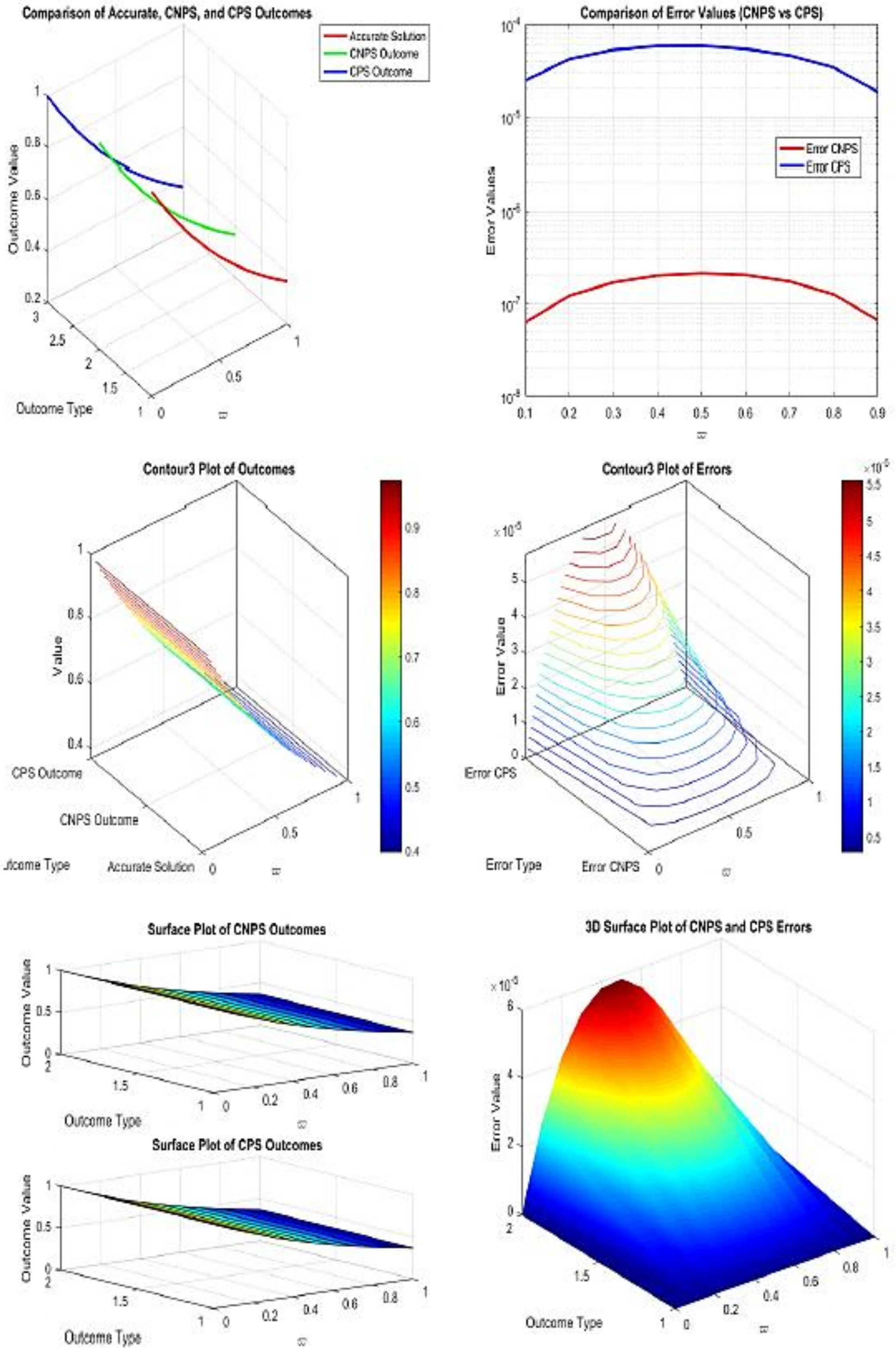

Fig. 2. Graphically representation of Accurate solution, CNPS outcome, CPS outcome and their Absolute Errors for problem 3.1 at $h = \frac{1}{10}$

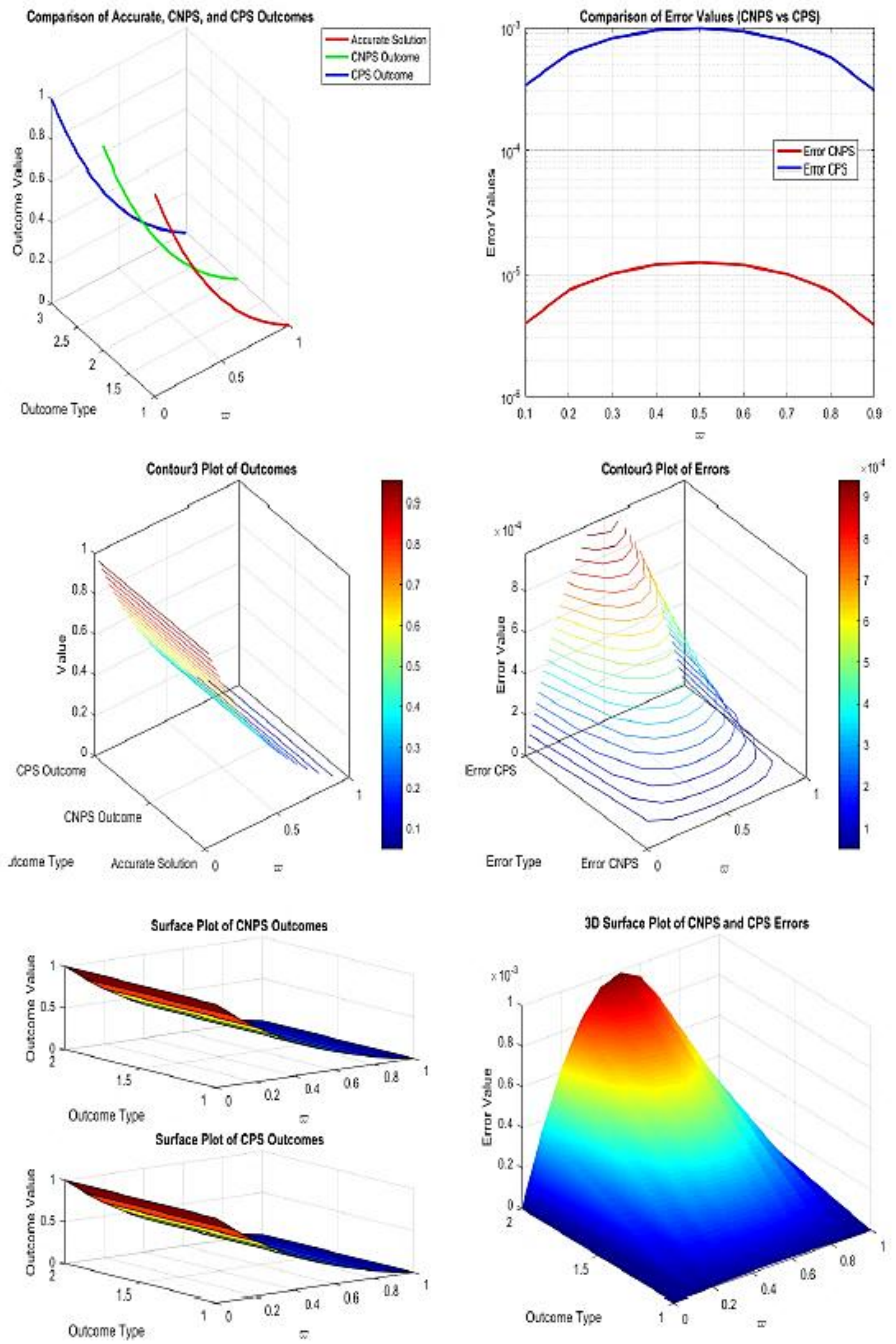

Fig. 4. Graphically representation of Accurate solution, CNPS outcome, CPS outcome and their Absolute Errors for problem 3.2 at $h = \frac{1}{10}$

DOI 10.2478/ama-2025-0021

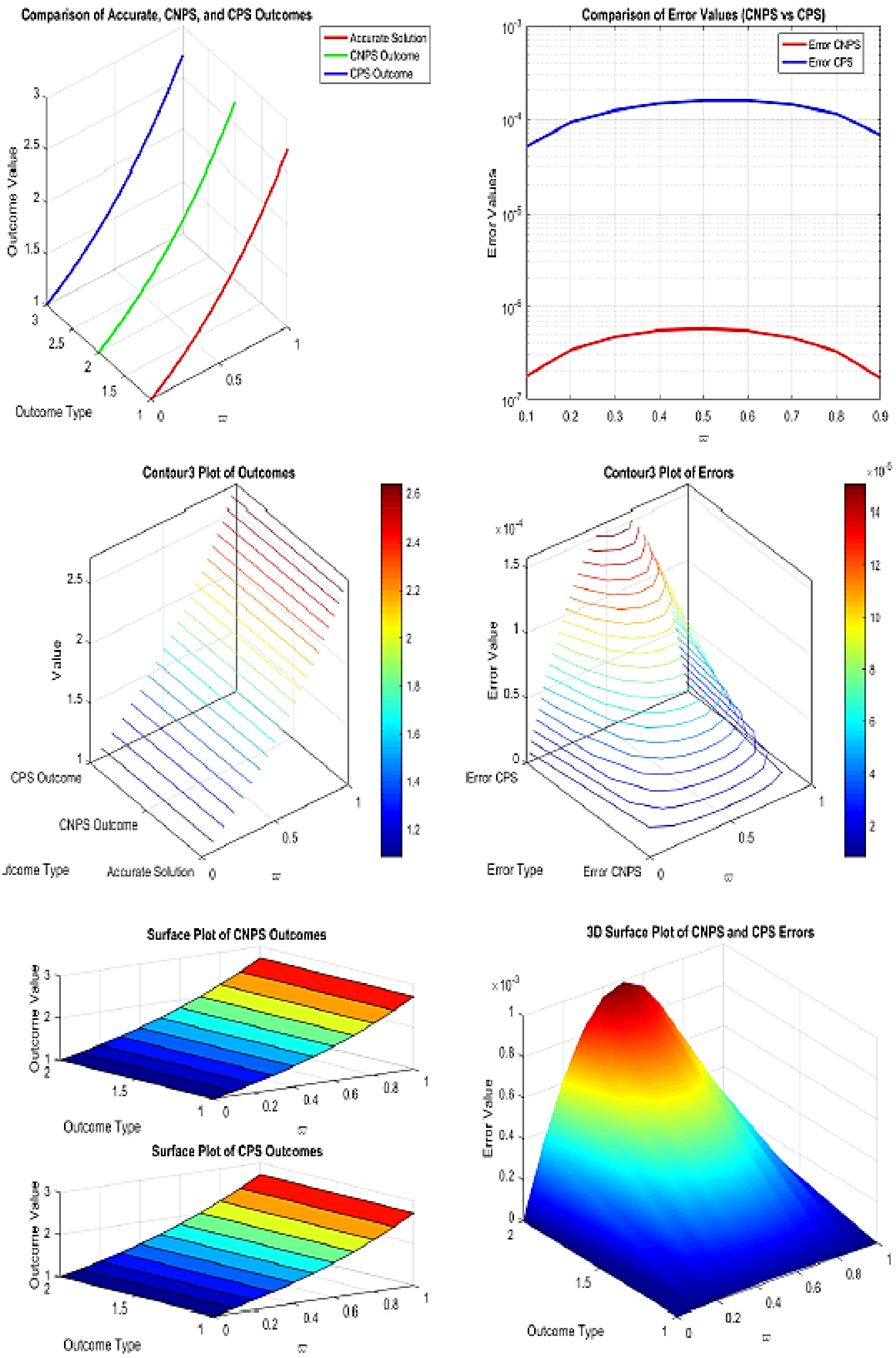

Fig. 6. Graphically representation of Accurate solution, CNPS outcome, CPS outcome and their Absolute Errors for problem 3.3 at $h = \frac{1}{10}$

Tab. 5. Comparison of accurate, CNPS along with CPS for problem 3.3 at $h = \frac{1}{10}$

ϖ	Accurate solution	CNPS solution	$\|error\|$ on CNPS	CPS solution	$\|error\|$ on CPS	[6]
0	1	1	1	0.00E-00	0.00E-00	0.00E-00
0.1	1.105170918	1.105171098	1.105120542	5.04E-05	1.80E-07	3.82E-06
0.2	1.221402758	1.221403102	1.221310719	9.20E-05	3.43E-07	1.35E-05
0.3	1.349858808	1.349859281	1.349734356	1.24E-04	4.73E-07	2.64E-05
0.4	1.491824698	1.491825254	1.49167782	1.47E-04	5.56E-07	3.85E-05
0.5	1.648721271	1.648721853	1.648562907	1.58E-04	5.82E-07	4.64E-05
0.6	1.8221188	1.82211935	1.821961083	1.58E-04	5.50E-07	4.70E-05
0.7	2.013752707	2.01375317	2.01360923	1.43E-04	4.62E-07	3.94E-05
0.8	2.225540928	2.225541259	2.225427036	1.14E-04	3.31E-07	2.48E-05
0.9	2.459603111	2.459603282	2.45953623	6.69E-05	1.70E-07	8.50E-06
1	2.718281828	2.71828	2.71828	0.00E-00	0.00E-00	0.00E-00

Tab. 6. Comparison of accurate, CNPS along with CPS for problem 3.3 at $h = \frac{1}{5}$

ϖ	Accurate solution	CNPS solution	$\|error\|$ on CNPS	CPS solution	$\|error\|$ on CPS	[6]
0	1	1	0.00E-00	1	0.00E-00	0.00E-00
0.2	1.221402758	1.221403377	6.19E-07	1.22103274	3.70E-04	5.42E-05
0.4	1.491824698	1.491825707	1.01E-06	1.491234204	5.90E-04	1.53E-04
0.6	1.8221188	1.822119714	9.13E-07	1.821484771	6.34E-04	1.95E-04
0.8	2.225540928	2.225541357	4.28E-07	2.225083141	4.58E-04	1.04E-04
1	2.718281828	2.71828	0.00E-00	2.71828	0.00E-00	0.00E-00

4. CONCLUSION

This paper addresses a gap in the existing literature by focusing on high-order nonlinear BVPs, which are less commonly explored compared to lower-order problems. this paper propose novel numerical strategies that involves non-polynomial and polynomial cubic splines to solve the nonlinear seventh order BVPs. Non-polynomial splines offer local control and are ideal for modeling intricate curves. In contrast, cubic polynomial splines excel in providing smooth interpolation. The choice between them depends on the problem's demands for local control or smoothness. The study shows that both CPS and CNPS methods can effectively solve nonlinear seventh-order BVPs, providing accurate approximations compared to exact solutions. For both methods, the domain $[0,1]$ is divided into sub-intervals with step sizes of $h = 1/10$ and $h = 1/5$.

The employed methods are rigorously assessed through experimentation on three distinct test problems. These benchmark problems encompass various nonlinear differential equations with different combinations of exponential, trigonometric, and polynomial terms, providing a diverse set of challenges for assessing the performance of the CPS and CNPS methods. The outcomes attained showcase an exceptional level of accuracy, extending up to 7 decimal places. These commendable results are vividly depicted in both the tabulated data and accompanying graphs. Such a high degree of precision substantiates the dependability and efficiency of the proposed method.

The CNPS method generally produces more accurate results than the CPS method. Smaller step sizes result in more accurate solutions for both methods, though at the cost of increased computational effort. For instance, with $h = 1/10$, the errors in both methods decrease compared to $h = 1/5$. Tab.1 shows that for Problem 3.1 with $h = 1/10$, the CNPS method achieves maximum absolute errors as low as 1.22×10^{-7}, while the CPS method has errors up to 5.83×10^{-5}. Tab.2 for $h = 1/5$ indicates that while both methods' errors increase, CNPS still outperforms CPS in accuracy.

The graphical illustrations (Fig. 2, 4, 6) highlight the precision of both methods. CNPS shows smaller absolute errors compared to CPS, indicating better convergence to the exact solution. Figure 1 visually confirms the superior accuracy of CNPS with lower absolute errors compared to CPS. Fig. 1, 3 and 5 shows the graphical comparison on CPS and CNPS with other spline [6].

By comparing the CPS and CNPS methods, the research highlights the strengths and weaknesses of each approach, offering valuable insights for future applications. This is illustrated through various figures and numerical simulations presented in the results section, demonstrating the close agreement between the numerical and exact solutions. This comparative analysis is particularly useful for researchers and practitioners seeking efficient numerical methods for similar problems.

REFERENCES

1. Ahmad B, Perviz A, Ahmad MO, Dayan F. Solution of Parabolic Partial Differential Equations Via Non-Polynomial Cubic Spline Technique. Scientific Inquiry and Review. 2021; 5(3): 60-76.
2. Chawla MM, Chawla V. A cubic B-spline solution of a seventh-order boundary value problem. International Journal of Numerical Analysis and Modeling. 2015; 12(4): 689-703.
3. Fang S, Ma X, Qu J, Zhang S, Lu N, Zhao X. (2020). Trajectory planning for seven-DOF robotic arm based on seventh degree polynomial. In Proceedings of 2019 Chinese Intelligent Systems Conference. 2020; Volume II 15th: 286-294. Springer Singapore.
4. Iqbal MJ, Rehman S, Pervaiz A, Hakeem A. Approximations for linear tenth-order boundary value problems through polynomial and non-

DOI 10.2478/ama-2025-0021

polynomial cubic spline techniques. Proc. Pakistan Acad. Sci. 2015; 52(4): 389-396.
5. Inc M, Akgül A. Numerical solution of seventh-order boundary value problems by a novel method. In Abstract and Applied Analysis; 2014; Hindawi.
6. Khalid A, Rehan A, Nisar KS, Osman MS. Splines solutions of boundary value problems that arises in sculpturing electrical process of motors with two rotating mechanism circuit. Physica Scripta. 2021; 96(10): 104001.
7. Kalyani P, Lemma MN. Solutions of seventh order boundary value problems using ninth degree spline functions and comparison with eighth degree spline solutions. Journal of applied Mathematics and physics. 2016; 4(02): 249.
8. Khazaei M, Karamipour Y. Numerical Solution of the Seventh Order Boundary Value Problems Using B-Spline method; 2021. arXiv preprint: 2109.06030.
9. Mabood F, Idrees M. Homotopy perturbation method and seventh-order boundary value problems. International Journal of Applied Mathematical Research. 2013; 2(1): 70-75.
10. Nikkar A, Dehghan M. A numerical technique for solving seventh-order boundary value problems using quartic B-spline functions. Applied Mathematics and Computation. 2013; 219(19): 9810-9820.
11. Pervaiz A, Ahmad A, Zafar Z, Ahmad MO. numerical solution of sixth order BVPs by applying non-polynomial spline method. Pakistan Journal of Science. 2014; 66(2):110.
12. Opanuga AA, Okagbue HI, Edeki SO, Agboola OO. Differential transform technique for higher order boundary value problems. Modern Applied Science. 2015; 9(13): 224-230.
13. Opanuga A, Owoloko E, Agboola O, Okagbue H. Application of homotopy perturbation and modified Adomian decomposition methods for higher order boundary value problems; 2017.
14. Rasekh M. An efficient numerical algorithm for solving seventh-order boundary value problems using cubic B-spline functions." Journal of Computational and Applied Mathematics. 2016; 297: 143-154.
15. Ramadan MA, Lashien IF, Zahra WK. Quintic nonpolynomial spline solutions for fourth order two-point boundary value problem. Communications in Nonlinear Science and numerical Simulation. 2009; 14(4): 1105-1114.
16. Rashidinia J, Khazaei M, Nikmarvani H. Spline collocation method for solution of higher order linear boundary value problems. TWMS J. Pure Appl. Math. 2015; 6(1): 38-47.
17. Richards G, Sarma P. (1994). Reduced order models for induction motors with two rotor circuits. IEEE Transactions on Energy Conversion. 1994; 9(4): 673-678.
18. Rubin S, Khosla P. (1976). Higher-order numerical solutions using cubic splines. AIAA Journal. 1976;14(7): 851-858.
19. Siddiqi SS, Iftikhar M. Variational iteration method for the solution of seventh order boundary value problems using He's polynomials. Journal of the Association of Arab Universities for Basic and Applied Sciences. 2015; 18: 60-65.
20. Siddiqi SS, Akram G, Iftikhar M. Solution of seventh order boundary value problems by variational iteration technique. Applied Mathematical Sciences. 2012; 6(94): 4663-4672.
21. Siddiqi SS, Iftikhar M. Solution of seventh order boundary value problems using Adomian decomposition method; 2013. arXiv preprint arXiv:1301.3603.
22. Singh R, Pandey RK, Singh A. An efficient approach to solve seventh-order boundary value problems using cubic trigonometric B-spline. Journal of Computational and Applied Mathematics. 2020;367: 112418.
23. Taiwo OA, Ogunlaran OM. A non-polynomial spline method for solving linear fourth-order boundary value problems; 2011.

Aasma Khalid and Rubab Batool are highly thankful to Government College Women University Faisalabad. Dr. Kashif Ali Abro is highly grateful to Mehran University of Engineering and Technology, Jamshoro and Mr. Akmal Rehan is highly thankful to University of Agriculture Faisalabad, Pakistan for generous support and facilities of this research work.

Aasma Khalid: https://orcid.org/0000-0003-4918-9732

Rubab Batool: https://orcid.org/0009-0000-2073-419X

Kashif Ali Abro: https://orcid.org/0000-0003-0867-642X

Akmal Rehan: https://orcid.org/0000-0001-9384-0743